Proceedings of the ASME 2020 International Design Engineering Technical Conferences & Computers and Information in Engineering Conference
IDETC/CIE 2020
August 16-19, 2020, St. Louis, MO, USA

DETC2020-22704

CONSTRAINT-BASED ANALYSIS OF PARALLEL KINEMATIC ARTICULATED WRIST MECHANISMS

Revanth Damerla* and Shorya Awtar
Precision Systems Design Laboratory
Mechanical Engineering, University of Michigan
Ann Arbor MI 48109

ABSTRACT

This paper presents a systematic constraint-based analysis of the motion attributes of six parallel kinematic articulated wrist mechanisms from the existing literature. These motion attributes include the number, nature (i.e. pure rotation, or translation, or a combination), and location of mechanism's Degrees of Freedom (DoFs) in the nominal and displaced configurations, range of operation along these DoFs, load transmission capability along these DoFs, and load bearing capability along the constraint directions. This systematic analysis reveals performance tradeoffs between these motion attributes for a given mechanism, as well as design tradeoffs across these multiple mechanisms with respect to these motion attributes. This analysis should help inform the suitability of a given mechanism for specific applications.

1. INTRODUCTION AND BACKGROUND

Articulated wrist mechanisms offer at least two rotations (commonly designated as pitch and yaw) and are used in a wide range of applications that require dexterous manipulation, remote access, or orientation adjustment. These applications include minimally invasive surgery [1–4], industrial operations such as robotic welding and spay-painting [5,6], handling of hazardous material [5,6], varying the orientation of a camera or other sensor in commercial [4,7–9] or aerospace applications [10,11], and varying the pointing angle of a fire retardant [12], to name a few. This wide range of applications has led to many unique articulated wrist mechanisms with various motion attributes, which determine the suitability of a mechanism for a given application.

These motion attributes include the Degrees of Freedom (DoFs) and Degrees of Constraint (DoCs) of an End Effector of a mechanism with respect to its Base (Fig. 1). DoFs are the independent directions of motion that the End Effector can undergo while DoCs are the independent directions that the End Effector is constrained to not move along. DoFs are geometrically represented by Freedom lines that capture pure rotation, pure translation, or a combination (i.e. screw). Similarly, DoCs are represented by Constraint lines that capture translational constraint, rotational constraint, or a combination (i.e. wrench). The freedom lines of a mechanism altogether form its freedom space, and similarly all the constraint lines of a mechanism form its constraint space. The freedom and constraint spaces of a mechanism define how it moves and transmits loads.

Freedoms and constraints follow certain basic rules of geometry: freedoms add in series, constraints add in parallel, and they are complementary to each other. The latter, also known as the Rule of Complementary Patterns [13], states that if there are *n* independent constraint lines, then there will be 6-*n* independent freedom lines, each of which will intersect every constraint line. Thus the freedom and constraint spaces are complementary. This rule can be used to identify freedom spaces from constraint spaces and vice versa. Screw theory provides a mathematical representation of the same concepts and associated tools, which are beneficial in cases where the constraint and freedom spaces are challenging to visualize and analyze using straightforward geometric arguments [14,15]. The Freedom and Constraint Topology (FACT) framework builds upon these geometric and mathematical principles to provide a comprehensive catalog of

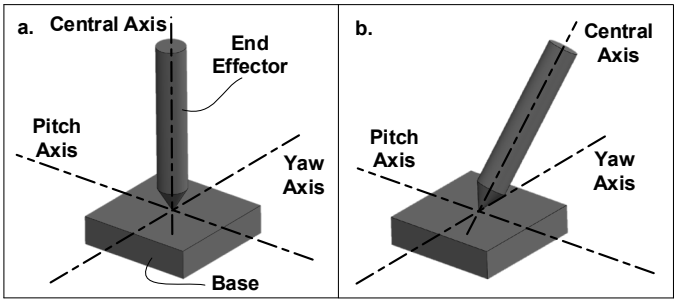

Fig.1 Generic Articulated Wrist Mechanism: a. Nominal configuration, b. Displaced configuration

Copyright © 2020 by ASME

all possible constraint and freedom spaces [16,17]. In this paper, we will make use of these geometric and mathematical tools, as needed, to analyze freedom and constraint spaces.

An articulated wrist mechanism offers at least two rotational DoFs (pitch and yaw) between an End Effector and Base, as generically shown in Fig. 1. Depending on the application, the mechanism can also have additional DoFs such as roll rotation or translation along the central axis. In an ideal scenario, at least in the nominal configuration, the two rotational DoFs (pitch and yaw) are pure rotations about their respective axes, which are orthogonal (Fig. 1a). However, upon displacement of the mechanism (Fig. 1b), i.e. when the End Effector and its associated central axis displaces relative to the Base, the pitch and yaw rotational DoFs can potentially change in location and nature. These motion attributes, among others, impact the performance and suitability of an articulated wrist mechanism for a given application, and are compiled below to capture the scope of investigation in this paper.

1. *Number of DoFs of the End Effector with respect to (w.r.t.) the Base in the nominal and displaced configurations.* The mechanism may exhibit redundant constraints in the nominal configuration that become non-redundant in the displaced configuration, or vice versa, resulting in an unexpected or undesired change in the number of DoF (also known as singularity) as the mechanism displaces. This can impact the range of motion of the mechanism as well as utility of the mechanism.
2. *Location of the DoFs in the nominal and displaced configurations.* Change in location can mean that the two rotational DoF (pitch and yaw) are no longer in the same plane w.r.t. the End Effector as they were in the nominal configuration, or are no longer orthogonal, or no longer intersect at the same point as they did nominally, or no longer intersect at all, or a combination of these, etc. This implies that the center of rotation of the End Effector w.r.t. the Base may drift, the axes of rotation may drift, and that the End Effector tip may not trace a perfect hemisphere.
3. *Nature of the DoFs in the nominal and displaced configurations.* Change in nature can mean that the two DoF (pitch and yaw) no longer remain purely rotational, and instead have some translational component that is kinematically tied to the rotations (i.e. screw motion). This implies that the End Effector may not have a pure rotation w.r.t. the Base and instead may also translate. As a result, it may not trace a perfect hemisphere.
4. The articulated wrist mechanism is intended to bear loads along its DoC directions, and therefore *load bearing capability (or equivalently stiffness)* in these directions is critical. This is impacted by the kinematics (e.g. transmission angles) and construction (e.g. joint or link stiffness) of the mechanism, which can change from the nominal to the displaced configuration.
5. If the articulated wrist mechanism is used in an active application i.e. actuation loads are transmitted from inputs on the mechanism (e.g. yaw input and pitch input) to the End Effector output, then *load transmission capability (or equivalently transmission stiffness)* becomes critical. This is also impacted by the kinematics and construction of the mechanism, and can change from the nominal to the displaced configuration.

The above motion attributes typically deviate from nominal behavior with increasing displacement of the mechanism, thereby creating a performance tradeoff between these attributes and range of motion. Additionally, the range of motion is also impacted by practical considerations such as size of links and joints in the mechanism and collisions between them.

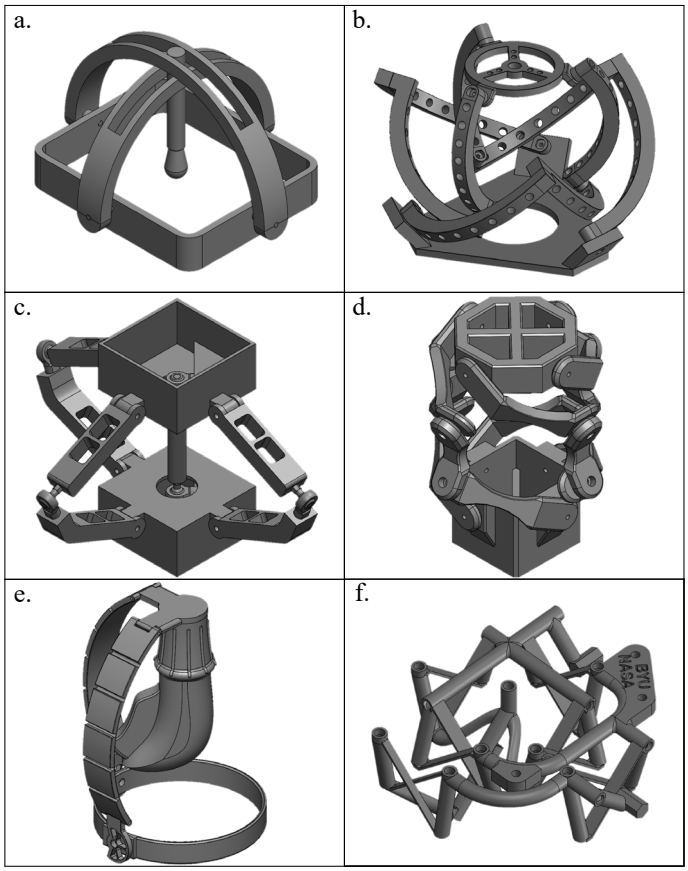

Fig. 2 Parallel Kinematic Articulated Wrist Mechanisms: a. Dual Arch, b. Agile Eye, c. OmniWrist V, d. OmniWrist III, e. FlexDex, f. BYU Space Pointing Mechanism

An articulated wrist mechanism can be either serial kinematic or parallel kinematic in its architecture. Parallel kinematic mechanisms allow ground mounted actuators (or equivalent transmission elements) making them preferable in active applications. Also, parallel kinematic architectures can be more compact and lightweight resulting in faster speeds. However, their design and evaluation (qualitative as well as quantitative) is relatively more complex [18]. Because of these reasons along with their wide applicability, we focus on parallel kinematic articulated wrist mechanisms in this paper. We identify six mechanism designs from the literature (see Fig. 2) and present a systematic and comprehensive constraint-based analysis of their motion attributes, with the goal of generating insights into performance tradeoffs (within a given mechanism)

Copyright © 2020 ASME

and design tradeoffs (between the various mechanisms).

These mechanisms were chosen primarily for their diversity in architecture, performance, and applications. As a result, they provide a representative set of the design tradeoffs that a designer can expect within parallel kinematic articulated wrist mechanisms. The Dual Arch [2,3] (Fig. 2a) and the Agile Eye [7,8] (Fig. 2b) mechanisms are composed entirely of rigid joints and links. Both these designs offer ideal rotational DoF attributes in that the yaw and pitch DoF remain in their nominal plane and retain their nominal intersection point even after displacement. The next two mechanisms are the OmniWrist V [19] (Fig. 2c) and the OmniWrist III [12,20,21] (Fig. 2d), which are also entirely composed of rigid links and joints. However, their pitch and yaw rotational DoF do not stay in the nominal plane upon displacement. The FlexDex® mechanism [1,2] (Fig. 2e) has some links and joints that are rigid and some that are compliant. Under the assumption of finite compliance along certain DoCs, this mechanism is also shown to offer yaw and pitch DoFs. The BYU Space Pointer mechanism [10] (Fig. 2f) is a novel monolithic design composed of rigid links and compliant joints, and makes intentional use of compliance to provide yaw and pitch DoFs, which do not retain their nominal behavior upon displacement.

2. CONSTRAINT-BASED ANALYSIS OF ARTICULATED WRIST MECHANISMS

The convention of illustrating constraints and freedoms used throughout this paper is as follows. Red dashed straight lines are used to indicate rotational freedoms while translational freedoms are shown as red dashed circles that are understood to be of infinite radius. The direction of translation is along the line normal to the plane of this circle. Screws are shown as solid green lines and constraints are shown as solid blue lines. Black center lines are used occasionally to denote axes of interest, but do not indicate any freedoms or constraints. Letters F and C denote freedoms and constraints, respectively, and numbers provide further specification. For example, $F1_2$ represents the second freedom offered by the first serial chain in the parallel kinematic mechanism. Unless otherwise specified, all links and joint are assumed to be ideal – the links infinitely rigid (or stiff), the joints are infinitely stiff and have zero error motions in their DoC directions, and the joints have zero stiffness and no motion restriction in their DoF directions.

2.1 Dual Arch Mechanism

The dual arch design (Fig. 3a) consists of two identical serial chains. The first chain is made up of a revolute joint R1 that connects the Base to the Arch Link L1; a sliding joint J1 connects Arch Link L1 to the End Effector. The freedom and constraint spaces of this first chain are shown in Fig. 3b. The revolute joint R1 provides the rotational freedom $F1_1$. Sliding joint J1 provides a total of four DoFs. The first is $F1_2$, which lies normal to the plane P1 that runs along the length of the sliding joint J1. $F1_3$ is a translation along the axis of R1, while $F1_4$ is a translation along the central axis of the End Effector. The final rotation, $F1_5$, is collinear to the central axis of the End Effector. The first chain therefore contributes one constraint, $C1_1$, as dictated by the Rule of Complementary Patterns, to the overall mechanism. This constraint line is parallel to $F1_2$, $F1_3$, and $F1_4$ and passes through the intersection of $F1_1$ and $F1_5$.

Fig. 3c illustrates the freedom and constraint spaces of the first chain when the arch has been rotated about the revolute joint R1. While $F1_1$ and $F1_3$ do not move, the freedoms $F1_2$ and $F1_4$ rotate to maintain their relationships to plane P1 and the End Effector, respectively. $F1_5$ also rotates with the End Effector. The resulting constraint $C1_1$ in the displaced configuration remains parallel to $F1_2$, $F1_3$, and $F1_4$ and passes through the intersection of $F1_1$ and $F1_5$.

The second chain is orthogonal to the first chain in placement but identical in structure, and therefore has analogous freedom and constraint spaces. The revolute joint R2, between the Base and Arch Link L2 in the second chain, has an axis that passes through the intersection of the R1 axis and the End Effector central axis. The constraint $C2_1$, contributed by the second chain, therefore intersects $C1_1$ at the same point as the intersection point of the R1 and R2 revolute joint axes (illustrated in black). The constraint and freedom spaces of the entire mechanism when the End Effector has been rotated in both pitch and yaw are shown in Fig. 3d. In this configuration, the two constraint lines $C1_1$ and $C2_1$ for the overall mechanism continue to intersect at the intersection point of the R1 and R2 joint axes. As a result, three independent freedoms F_1, F_2, and F_4 for the overall mechanism also pass through this intersection point. When these three freedoms are not coplanar, they form the same freedom space as an ideal spherical joint. Another freedom line, F_3, lies in the plane normal to the central axis of the end effector. This line can be moved to a point infinitely far away to represent translation of the End Effector along the central axis of the End Effector. Therefore, this mechanism, in the illustrated form, offers 4 DoFs.

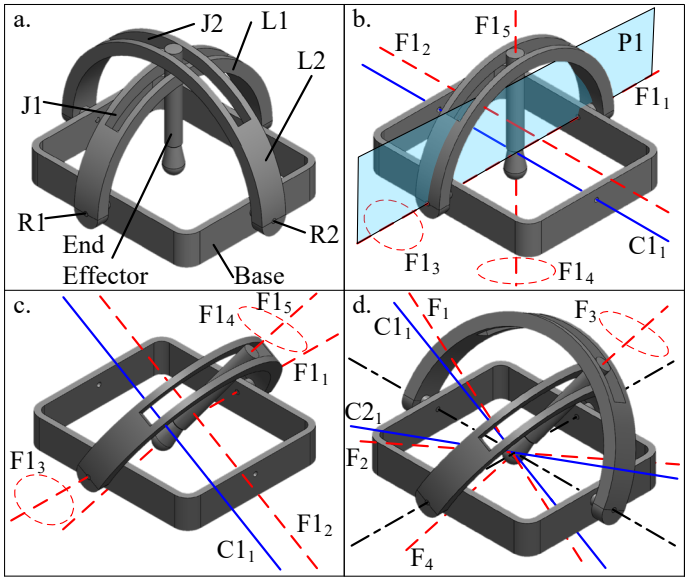

Fig. 3 Dual Arch: a. Full mechanism nominal configuration, b. First chain nominal configuration, c. First chain displaced configuration, d. Full mechanism displaced configuration

Copyright © 2020 ASME

Freedom F_3 can be removed by constraining the End Effector w.r.t. either or both Arch Links in translation along the central axis. Freedom F_4 can be removed by introducing a rotational constraint between the End Effector and only one of the sliding joints. With these additional constraints in place, F_1 and F_2, the two remaining freedoms, still lie in the plane normal to the central axis of the End Effector in any displaced configuration. The intersection point of these two freedoms also does not drift from the intersection point of R1 and R2 axes.

A key benefit of this mechanism its relatively compact and simple structure. However, range of motion is limited by singular configurations when either of the two Arch Links reaches 90° in any direction. When the mechanism is increasingly articulated in one rotational DoF, the approaching singularity causes a loss in transmission ratio in the other rotational DoF. This means that End Effector can no longer be actuated along the second DoF. As the transmission ratio drops, the mechanical advantage goes up, which can be beneficial for load transmission. This is because when the mechanism is articulated in one DoF, the moment arm from the revolute joint associated with the second DoF to the point of contact between the second Arch Link and End Effector becomes smaller. As a result, an input torque at the second DoF can support a larger force at the End Effector. Load bearing capabilities along the DoCs are similarly affected as the mechanism moves from its nominal to a displaced configuration. When mechanism is articulated in one DoF (e.g. corresponding to R1 joint), the translational DoC along the R1 axis becomes stronger because the End Effector moves closer to the base and therefore the R2 joint axis that supports this DoC. The mechanism's physical limitations (i.e. collisions) and ultimately singularities prevent it from tracing out an entire hemisphere but it can trace out a section of this hemisphere around the nominal configuration. Within this continuous but finite range of motion, the load transmission and bearing capabilities are dictated more by the geometry and construction of the various rigid links and joints, which can be designed to suit the application. A practical manufacturing consideration for this mechanism is the long sliding contact required between the End Effector and Arch Links. Furthermore, this mechanism offers a large open space around the intersection of the pitch and yaw axes, making this mechanism suitable not only for pointing and tracking applications, but also applications that require a remote center of rotation located in an open space [2,3].

2.2 Agile Eye Mechanism

The Agile Eye mechanism is representative of a class of 3-RRR mechanisms that are spherical 3-DOF parallel kinematic manipulators capable of pitch, yaw, and roll rotations. Numerous other examples of mechanisms with the same kinematic architecture exist within the literature [22,23]. However, the Agile Eye stands apart because its geometry enables a relatively large workspace [24].

This mechanism is composed of three identical serial chains. The structure of the first serial chain, highlighted in pink, is shown in Fig. 4a. Revolute joint $R1_1$ connects the Base to the first link $L1_1$, which is made up of two circular arc sections that are rigidly connected. $R1_2$ connects $L1_1$ to $L1_2$, which is made up of only one circular arc section. Finally, $R1_3$ connects $L1_2$ to the End Effector. The most important physical detail of this mechanism is that the axes of rotation of all nine revolute joints always intersect the same point in space regardless of displacement. The constraint and freedom spaces of the first chain in the nominal and displaced configuration are shown in Figs. 4b and 4c, respectively. In both cases, $F1_1$, $F1_2$, and $F1_3$ intersect the same point but are not coplanar; this chain and therefore the mechanism becomes singular if this condition is not met. The freedoms create a corresponding constraint space with three constraint $C1_1$, $C1_2$, and $C1_3$ that also intersect the same point and are not coplanar. Since the freedom lines of all three chains share the same intersection point, there are six redundant constraints. The resulting constraint and freedom spaces of the entire mechanism in the displaced configuration are shown in Fig. 4d. Since the mechanism's freedom space comprises three pure rotational freedom lines that share the same intersection point and are not coplanar, it behaves like an ideal spherical joint. This freedom space remains unchanged throughout the mechanism's workspace [7,24].

The strict geometric requirement of joint DoFs intersecting at the same point and complex intertwined architecture that are required in this mechanism place unique practical limitations on its performance. Apart from any singularities, the reachable workspace in all three DOFs is dictated by collisions between the links and is therefore inversely related to their size (e.g. thickness). Similarly, load transmission and load bearing capabilities are directly related to the size and stiffness of the links. For applications that do not require very high load bearing or transmission capabilities, this mechanism has been shown to achieve a workspace of 140° cone of constant radius with ±30° in roll [7]. When only pitch and yaw are required, one can either actuate all three inputs in a coordinated manner to achieve the two desired rotations, or one can freeze one of the three inputs.

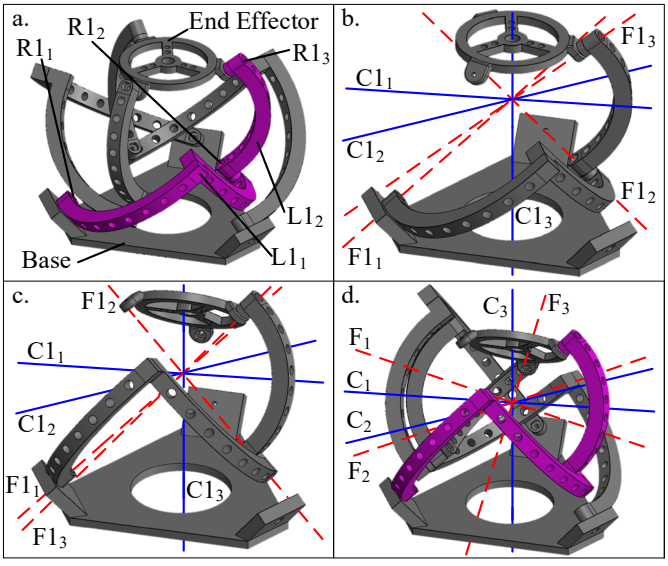

Fig. 4 Agile Eye: a. Full mechanism nominal configuration b. First chain nominal configuration, c. First chain displaced configuration, d. Full mechanism displaced configuration

Copyright © 2020 ASME

This mechanism does not offer a large open space around the center of rotation (defined by the intersection of the two rotational DoF) over the entire range of motion. This makes this mechanism more suitable for fast pointing and tracking applications and less so for human interface applications.

2.3 OmniWrist V Mechanism

OmniWrist mechanisms are a series of designs that offer singularity-free articulation over large ranges of motion [5,9,19]. Of these, the OmniWrist V and VI have the simplest architecture; the former is shown in Fig. 5a and consists of two different types of chains. The first chain is an example of the outer chain. A revolute joint $R1_1$ connects the Base to link $L1_1$. A spherical joint $S1_1$ connects link $L1_1$ to link $L1_2$ which is connected to the End Effector via revolute joint $R1_2$. The fourth chain in the mechanism is the central chain. It consists of a spherical joint $S4_1$ that connects the Base to link $L4_1$ which is connected to the End Effector via spherical joint $S4_2$.

The freedom and constraint spaces of the first outer chain in the nominal configuration are shown in Fig. 5b. $R1_1$ provides the freedom $F1_1$, spherical joint $S1_1$ provides freedoms $F1_2$, $F1_3$, and $F1_4$, and $R1_2$ provides $F1_5$; this adds to a total of five DoFs. The corresponding constraint line $C1_1$ must pass through the center of $S1_1$ in order to intersect $F1_2$, $F1_3$, and $F1_4$. It also must run parallel to $F1_1$ and $F1_5$.

The freedom and constraint spaces of the central chain in the nominal configuration are shown in Fig. 5c. Both $S4_1$ and $S4_2$ provide three degrees of freedom. However, one of the DoFs is redundant and is represented by the shared DoF $F4_3$. The resulting single constraint line $C4_1$ is the line drawn between the centers of the two joints. This relation holds throughout the mechanism's workspace.

With an understanding of the constraints provided by each chain in the nominal configuration, the nominal mechanism constraint map can be drawn as shown in Fig. 5d. Since $C1_1$, $C2_1$, and $C3_1$ are coplanar in the nominal configuration, any two lines lying within the same plane and also intersecting $C4_1$ can be chosen. These lines do not have to be orthogonal and are only illustrated in this way for convenience. This freedom space represents pitch and yaw rotations and would appear to make this mechanism an excellent candidate in almost any application.

However, the freedom space changes once the mechanism has moved to any displaced configuration within its workspace because the constraint lines of the outer chains become more complicated. The freedom and constraint spaces for the first outer chain in the displaced configuration are shown in Fig. 5e. While links $L1_1$ and $L1_2$ become displaced, the relative orientations of freedoms $F1_1$, $F1_2$, $F1_3$, and $F1_4$ all remain the same as in the nominal configuration. However, the orientation of $F1_5$ rotates to maintain its relation to the displaced end effector. As a result, the constraint line $C1_1$ is more complicated to identify. First the plane $P1_1$ containing $F1_1$ and the center of $S1_1$ must be constructed. $C1_1$ is the line lying in this plane that intersects the center of $S1_1$ and the intersection of $P1_1$ with $F1_5$. This constraint line will naturally intersect $F1_1$ because it lies in $P1_1$ and therefore intersects every freedom line.

Since the constraint lines for the four chains are no longer in simple orientations, it is difficult to draw the corresponding freedom space. It is therefore simpler to use screw theory directly instead of using the geometric principles of constraint analysis. The constraint and freedom spaces of the OmniWrist V in the displaced configuration are shown in Fig. 5f. The freedom space now consists of two screw lines that appear to intersect each other and $C4_1$ at the same point. In addition, the plane comprising these two screw lines appears normal to the central axis of the End Effector and does not drift in any displaced configurations. However, given the numerical approach used to determine the freedom space, these attributes could not be confirmed geometrically. The FACT catalog helps identify that the corresponding constraint space is a circular hyperboloid.

The appearance of screw lines instead of pure rotational lines means that this mechanism is unable to trace out a perfect hemisphere. Nevertheless, this mechanism is a great candidate for pointing or tracking applications as well as for manufacturing applications such as welding and spray painting. In the latter applications, a robotic arm that supports the OmniWrist V can make up for the small positional changes caused by the screw freedoms. Actuation of this mechanism is typically done via rotation of the first links of two outer chains (e.g. $L1_1$ about the joint $R1_1$).

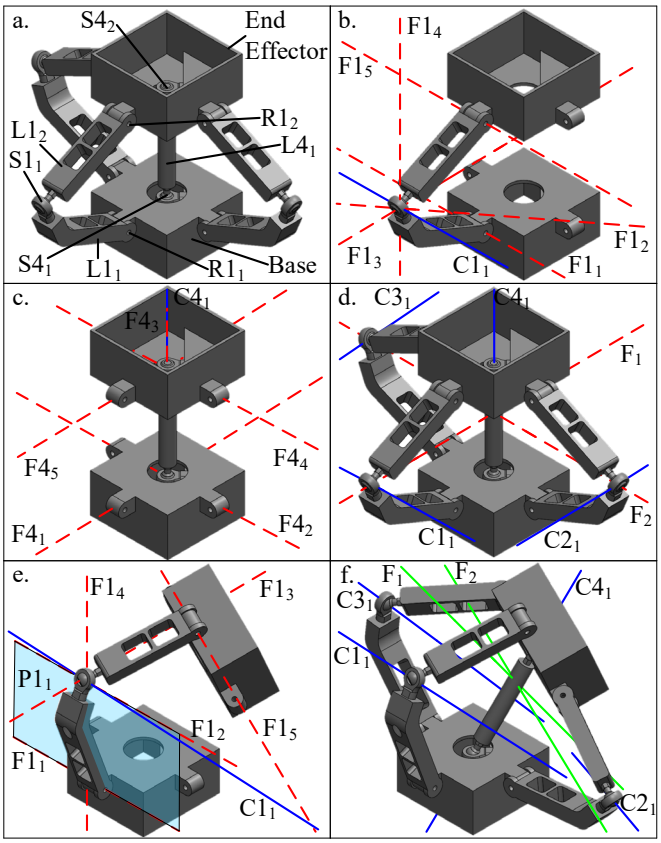

Fig. 5 OmniWrist V: a. Full mechanism nominal configuration, b. First outer chain nominal configuration, c. Central chain nominal configuration, d. Full mechanism nominal configuration, e. First chain displaced configuration, f. Full mechanism displaced configuration

Copyright © 2020 ASME

The mechanism can be actuated through its full 180° hemispherical range of motion with smaller rotations of the first links (i.e. large transmission ratio), which allows for the use of limited stroke rotary or linear actuators.

The central chain plays a critical role in the performance of this mechanism. The spherical joints $S4_1$ and $S4_2$ dictate the range of motion of the mechanism. For the End Effector to span its full hemispherical range, these spherical joints together have to provide 90° of rotation from their nominal configuration. The central chain also provides load bearing capability along the constraint $C4_1$.

In general, high load bearing along constraint directions can be achieved via adequately stiff links and joints in the mechanism because of few geometric limitations; links can be made thicker for little cost beyond additional mass. Large transmission ratio also leads to low mechanical advantage. It is therefore feasible to transmit large input actuation torque from the first links (e.g. $L1_1$) to the End Effector. It is also important to note that the outer chains in this mechanism can be spaced 120° apart instead of 90°. Furthermore, this architecture allows for the inclusion of additional outer chains without changing the freedom space of the mechanism. For example, the OmniWrist VI has a very similar structure compared to OmniWrist V but includes four outer chains instead of three [19]. The freedom space is preserved because, under ideal geometry, the constraint added by the additional outer chain is redundant in every displaced configuration. This can be confirmed via either geometric or mathematical analysis. Thus, while the OmniWrist VI requires tighter manufacturing and assembly tolerances to manage the over-constraint, it will have improved load bearing capabilities due to the additional stiffness of a fourth chain.

2.4 OmniWrist III Mechanism

While the OmniWrist III may appear architecturally different from the OmniWrist V, a constraint-based analysis reveals the similarities between these two mechanisms. In its most basic form, this mechanism consists of three identical chains that are wrapped around the End Effector. But as in the case of the OmniWrist V, additional chains can be added while preserving the freedom space and improving the load bearing and transmission capabilities. Accordingly, we present a four-chain version of the OmniWrist III in Fig. 6.

Each chain consists of three links connected by four revolute joints. The structure of the first chain, highlighted in pink, is shown in Fig. 6a. Revolute joint $R1_1$ connects the Base to link $L1_1$ and $R1_2$ connects this link to $L1_2$. $R1_3$ connects $L1_2$ to $L1_3$ which is connected to the End Effector via $R1_4$. It should be noted that $L1_1$ and $L1_3$ are identical links.

The freedom and constraint spaces of the first chain in the nominal configuration are shown in Fig. 6b. Each revolute joint in the chain provides the freedom with identical numbering. The most important feature of this mechanism is that $F1_1$ and $F1_2$ intersect at a point along the central axis of the base and $F1_3$ and $F1_4$ intersect at a point along the central axis of the end effector. This is possible because of the special construction of links $L1_1$ and $L1_3$; these two freedom intersections remain in the same location of the Base and end Effector regardless of mechanism orientation. The constraint line $C1_2$ is therefore the line that connects these two intersections. This line is very similar to the constraint line due to the central chain of the OmniWrist V. $F1_2$ and $F1_3$ also intersect at a point outside of the mechanism because of the special construction of $L1_2$. Constraint line $C1_1$ can be drawn by observing the similarities between the OmniWrist III chain's freedom space and the OmniWrist V outer chain's freedom space. The intersection of freedoms $F1_2$ and $F1_3$ mimic the freedom space of the OmniWrist V outer chain's spherical joint. $C1_1$ can be drawn with a line that passes through this freedom intersection and is also parallel to $F1_1$ and $F1_4$.

The constraint and freedom spaces of the overall mechanism in the nominal configuration are shown in Fig. 6c. The constraint space is identical to that of the OmniWrist V in the nominal configuration. C_5 is composed of the four redundant constraints $C1_2$, $C2_2$, $C3_2$, and $C4_2$. If the special link relations created by the geometry of the first and third links (e.g. $L1_1$ and $L1_3$) did not hold for all four chains, the four constraints would not be redundant and this mechanism would be unable to pitch or yaw. Since $C1_1$, $C2_1$, $C3_1$, and $C4_1$ are all coplanar, one of the constraints is redundant. The mechanism therefore has four independent constraints and produces a freedom space with lines F_1 and F_2 that are coplanar to $C1_1$, $C2_1$, $C3_1$, and $C4_1$ and intersect C_5. Thus, this mechanism also provides pure pitch and yaw rotational DoFs in the nominal configuration but does not maintain this freedom space in displaced configurations.

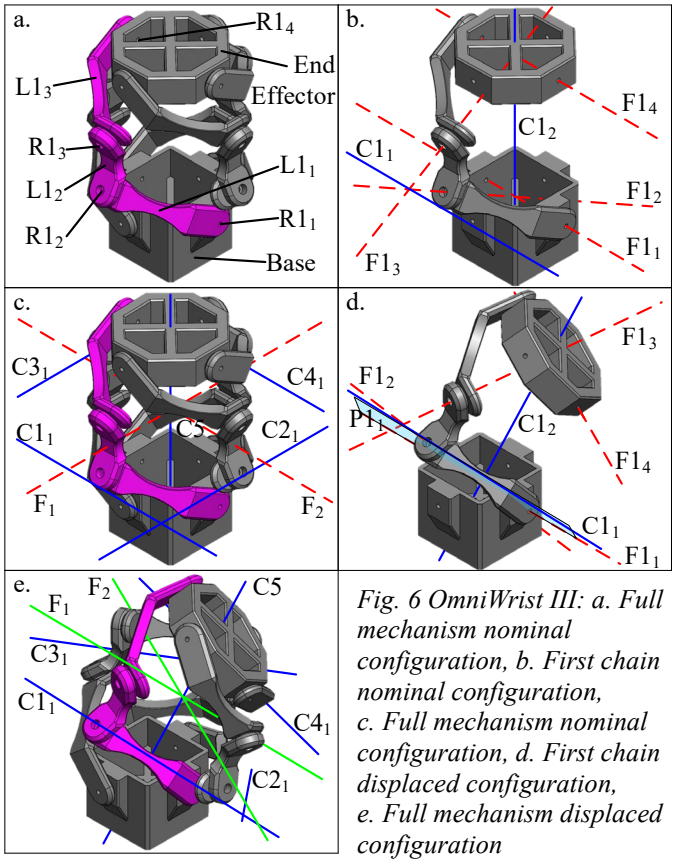

Fig. 6 OmniWrist III: a. Full mechanism nominal configuration, b. First chain nominal configuration, c. Full mechanism nominal configuration, d. First chain displaced configuration, e. Full mechanism displaced configuration

Copyright © 2020 ASME

The similarities between the two OmniWrist designs (V/VI and III) remain even when both are in displaced configurations. Fig. 6d shows the freedom and constraint spaces of the first chain in a displaced configuration. $F1_1$, $F1_2$, and $F1_3$ remain in similar orientations as in the nominal configuration while $F1_4$ rotates in order to maintain its relationship with the end effector. However, the intersection points of $F1_1$ and $F1_2$, $F1_2$ and $F1_3$, and $F1_3$ and $F1_4$ are preserved. As expected, $C1_2$ still passes through the same points on the Base and End Effector. In order to find $C1_1$, an analogous approach to what was used to find the constraint space of the outer chains in the OmniWrist V in the displaced configuration is used. First, the plane $P1_1$ that contains $F1_1$ and the point of intersection between $F1_2$ and $F1_3$ is constructed. $C1_1$ is the line lying in $P1_1$ that passes through the intersection point between $F1_2$ and $F1_3$ and intersects $F1_4$.

The constraint and freedom spaces of the mechanism in a displaced configuration are shown in Fig. 6e. C_5 still collectively represents the redundant constraints $C1_2$, $C2_2$, $C3_2$, and $C4_2$ and remains analogous to the constraint provided by the central chain in the OmniWrist V. The mechanism's freedom space is also composed of two screws that, based on numerical analysis, appear to intersect each other and remain perpendicular to the central axis of the End Effector. The intersection point also remains a constant distance from the End Effector, meaning that while the nature of the DoFs change, their location does not drift. As is the case with the OmniWrist V mechanism, these attributes of the freedom space were observed via a numerical analysis. In future, this may be proven geometrically as well. The FACT catalog helped identify the constraint space as a circular hyperboloid, as expected.

While the freedom and constraint spaces of the OmniWrist III and OmniWrist VI are similar, the performance tradeoffs of the two mechanisms are very different due to the significant differences in physical architecture. Because its freedom spaces comprises two intersecting screws, the OmniWrist III is also not able to trace out a perfect hemisphere but can trace out an oblong hemisphere (full 180º) while remaining free of singularity. Compared to OmniWrist V, the OmniWrist III has a unique aspect ratio – greater height and narrow width, which might be advantageous in certain tight-space applications. This mechanism can also be actuated via short-stroke rotary or linear actuators due to its high transmission ratio, which also corresponds to lower mechanical advantage.

The mechanism's range of motion is determined by collision between links from different chains. This results in a tradeoff between link dimensions (e.g. thickness) and the range of motion. To maximize range of motion, the links must be compact but this can also result in finite stiffness of the supposedly rigid links. This adversely impacts load bearing and transmission capabilities. In particular, the load bearing capability along constraint C_5 is compromised since it depends on the bending stiffness of the serially connected links (e.g. $L1_1$-$L1_2$-$L1_3$). This is in contrast to the OmniWrist V, where load bearing in this direction is dictated by the central chain. These features and tradeoffs make this mechanism a promising candidate in applications including pointing, tracking, and manufacturing.

2.5. FlexDex® Mechanism

The FlexDex mechanism offers constraint and freedom spaces that are similar to the Dual Arch mechanism, but highlights many advantages of compliant elements. The FlexDex mechanism is composed of two identical chains; the structure of the first chain is shown in Fig. 7a. Revolute joint $R1_1$ connects the Base to link $L1_1$ and revolute joint $R1_2$ connects $L1_1$ to $L1_2$. $L1_2$ is a compliant strip composed of alternating "rigid" sections and "compliant" hinges. These compliant hinges are initially modeled as ideal revolute joints; the first two of these joints, $H1_1$ and $H1_2$ are labeled in the figure. While an ideal revolute joint has zero motion and infinite stiffness along its constraint directions, in practice, a complaint hinge will have finite stiffness and parasitic error motion (especially under loading) along its constraint directions. Similarly, the rigid sections are modeled initially as being ideal, i.e. infinitely stiff. A Revolute joint $R1_3$ connects $L1_2$ to the End Effector.

The freedom and constraint spaces of the first chain in the nominal configuration are shown in Fig. 7b. Each revolute joint and compliant hinge provides a single DoF as expected. An important feature of link $L1_2$ is that the axis of rotation of each compliant hinge is parallel to those of $R1_2$ and $R1_3$. The compliant hinges therefore provide freedoms that are parallel to $F1_2$ and $F1_4$. However, only a maximum of three of these parallel freedoms are independent and multiple freedoms provided by compliant hinges have been omitted in the figure for simplicity of illustration. This relationship only holds when the compliant strip is not held flat. In this orientation, $F1_2$, $F1_3$, $F1_4$, and all other freedoms provided by the compliant strip are parallel and coplanar. This is a singular configuration because only two of these freedoms are independent. This issue is inherently avoided by the length and orientation of the two transmission strips in the FlexDex mechanism. In the non-singular configuration of the compliant strip, the first chain provides four freedoms – $F1_1$, $F1_2$, $F1_3$, and $F1_4$ – at the End-Effector. The corresponding constraint space is two lines $C1_1$ and $C1_2$ that are parallel to $F1_2$, $F1_3$, and $F1_4$ and intersect $F1_1$. While these two constraint lines must be coplanar with $F1_1$, the absence of a fifth freedom $F1_5$ in the first chain (which was present in the case of the Dual Arch Gimbal) removes the strict positional requirement for the constraints; they can lie anywhere in the plane they share with $F1_1$.

The constraint and freedom spaces of the overall mechanism in the nominal configuration are shown in Fig. 7c. Since the four constraints are coplanar, only three of these constraints are independent. This produces the corresponding freedom space with the three independent freedoms F_1, F_2, and F_3 that lie in the same plane with at most two that are parallel to each other. It is therefore possible to arrange these freedoms such that F_1 and F_2 correspond to pitch and yaw motions and F_3 corresponds to a vertical translation. This is the expected freedom space of an articulated wrist mechanism with an additional translational DoF. However, the freedom and constraint spaces deviate from this ideal arrangement in displaced configurations of the mechanism.

The freedom and constraint spaces of the first chain after the chain has rotated about $F1_1$ are shown in Fig. 7d. Freedoms $F1_2$,

Copyright © 2020 ASME

$F1_3$, and $F1_4$ rotate with their respective revolute joints and compliant hinges. $C1_1$ and $C1_2$ still intersect $F1_1$ but also rotate in order to remain parallel to $F1_2$, $F1_3$, and $F1_4$.

The constraint and freedom spaces of the overall mechanism after the first chain has rotated about $F1_1$ are shown in Fig. 7e. The mechanism constraint space now contains four constraints that do not lie in a single plane. There is therefore no longer any redundancy among the constraints. As a result, the mechanism's freedom space devolves into a 2 DOF space where the freedoms are parallel to C_3 and C_4 and intersect both C_1 and C_2. These two freedoms can be arranged so that F_1 corresponds to continued rotation about the same axis (i.e. $F1_1$) and F_2 corresponds to a translation along the central axis of the end effector. The loss of DoF is critical in this case because the mechanism is no longer an articulated wrist mechanism. However, note that this analysis, and therefore the resulting outcome, is based on an ideal constraint assumption for the compliant hinges and revote joints and ideal rigid sections and links.

In practice, the compliant strip is not ideal and compliance is advantageously employed to introduce intentional deviation from ideal behavior. In particular, the compliant "rigid" sections as well as the compliant hinges have finite compliance in torsion (as opposed to zero compliance or infinite stiffness in the ideal scenarios). This small but finite compliance of the compliant strip in torsion plays an important role in providing the desired articulation functionality in this mechanism, as demonstrated in practical use [1].

With this knowledge and some modified assumptions, we can rerun the freedom and constraint analysis. Most importantly, even though torsion is not truly a freedom direction for the compliant strip, we introduce the freedom line $F1_5$ due to the fact that the complaint strip is not ideal and has some small but finite compliance in this direction. With this assumption, the resulting freedom and constraint of the first chain with link $L1_2$ compliant in torsion after it has rotated about the freedom $F1_1$ is shown in Fig. 7f. This freedom space is identical to the freedom space of the first chain in the Dual Arch in a displaced configuration. The addition of the freedom $F1_5$ removes one of the two constraints that are present in Fig. 7d. In addition, $C1_1$ must now intersect the intersection of $F1_1$ and $F1_5$.

Making a similar "non-ideal" assumption for the second compliant strip, the constraint and freedom spaces of the overall mechanism after both chains have rotated about $F1_1$ and $F2_1$ respectively are shown in Fig. 7g. The mechanism freedom space now represents that of an articulated wrist mechanism as F_1 and F_2 correspond to pitch and yaw freedoms. In addition, these two freedoms do not drift because the constraints $C1_1$ and $C2_1$ cannot drift. F_3 represents translation of the end effector about its central axis as it did when the mechanism was in the nominal configuration. Freedom F_4 represents rotation of the end effector about its central axis, resulting from the torsional compliance assumption and associated additional freedom of both compliant strips. However, the stiffness of this rotation will still remain higher than in the directions of the other DoFs. Overall, intentional use of compliance is mechanism design highlights the limits of constraint analysis that assumes ideal links and joints.

While intentional compliance provides desired functionality and expands the mechanism design space, it also leads to an inherent set of tradeoffs. Increasing the above torsional compliance of the compliant strips reduces the load bearing and transmission capabilities of the mechanism. Transmission of an actuation load from the first revolute joints (e.g. $R1_1$) to the End Effector will cause the compliant strip to twist, thereby limiting its torque transmission capability. Also, such twisting means that the freedoms e.g. $F1_2$, $F1_3$, $F1_4$ provided by $L1_2$ will no longer be parallel. This will influence the number of DoFs of the mechanism as the freedoms provided by the compliant hinges will no longer be redundant. Similar issues will impact load bearing capabilities along the DoCs of the mechanism.

Furthermore, this mechanism stores energy because of its compliance thereby impacting transmission efficiency. However, with suitable optimization of compliance and link and joint dimensions, it is possible for this mechanism to achieve close to full hemispherical range of motion.

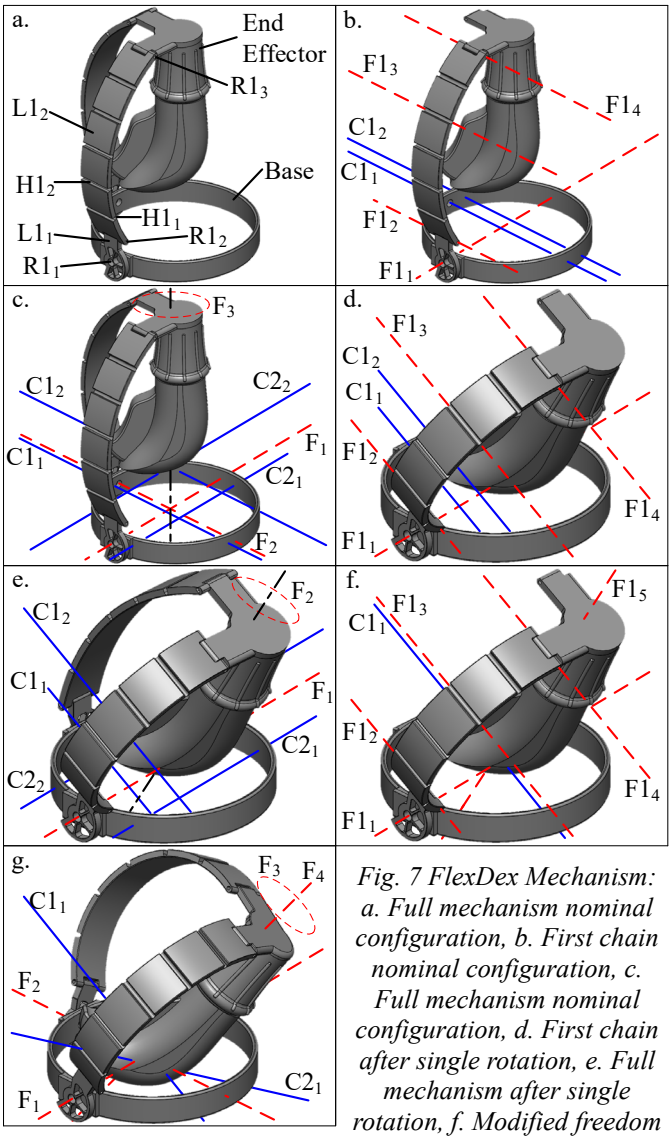

Fig. 7 FlexDex Mechanism: a. Full mechanism nominal configuration, b. First chain nominal configuration, c. Full mechanism nominal configuration, d. First chain after single rotation, e. Full mechanism after single rotation, f. Modified freedom space for first chain after single rotation, g. Full mechanism after both rotations

Copyright © 2020 ASME

Like the Dual Arch mechanism, the FlexDex mechanism offers a large open space around the center of rotation (i.e. intersection of F_1 and F_2). This makes this mechanism well suited for applications that require a human interface [1,2].

2.6 BYU Space Pointing Mechanism

The Space Pointing Mechanism offers a unique and novel monolithic compliant parallel kinematic architecture [10], shown in Fig. 8a in its nominal configuration. It contains two chains shown in pink and blue that are not identical. A rotary actuator is meant to be connected to each chain via the hexagonal protrusions labeled M1 and M2. The first chain, shown in pink, contains four cross-axis flexural pivots, which are meant to approximate revolute joints. M1 is connected to the first two pivots $H1_1$ and $H1_2$ via rigid link L1. $H1_1$ and $H1_2$ have collinear axes of rotation. These two flexural pivots are directly connected to the Base, shown in gray. Link L1 connects M1, $H1_1$, and $H1_2$ to the other two flexural pivots $H1_3$ and $H1_4$. $H1_3$ and $H1_4$ also have collinear axes of rotation. These two pivots are directly connected to the End Effector, shown in orange. The second chain, shown in blue, consists of two cross-axis flexural pivots $H2_1$ and $H2_2$ as well as one split-tube flexure $H2_3$, which also approximates a revolute joint about its axis. It is important to note that $H2_3$ passes underneath $H2_2$. The Base is directly connected to $H2_1$, which is connected to M_2 via rigid link L2. L2 is also connected to $H2_2$. $H2_3$ is directly connected to both $H2_2$ and the End Effector.

The freedom and constraint spaces of the first chain in the nominal configuration are shown in Fig. 8b. Freedom $F1_1$ is provided by both $H1_1$ and $H1_2$ and $F1_2$ is provided by both $H1_3$ and $H1_4$. These two freedoms are orthogonal and intersect along the central axis of the End Effector. The corresponding constraints include three constraints $C1_1$, $C1_2$, and $C1_3$ that are not all coplanar and intersect at the intersection of the two freedoms. $C1_4$ is coplanar to both freedoms but does not intersect at their intersection. The freedom and constraint spaces therefore provide for an articulated wrist mechanism.

The freedom and constraint spaces of the second chain in the nominal configuration are shown in in Fig. 8c. Each of the flexural joints $H2_1$, $H2_2$, and $H2_3$ provide an independent freedom line, $F2_1$, $F2_2$, and $F2_3$, respectively. This is because while the three freedoms intersect at the same point, $F2_3$ does not lie in the same plane as the other two freedoms. This intersection point is the same point of intersection for the two freedoms from the first chain. In addition, $F2_1$ and $F2_2$ are coplanar to both of these freedoms and collinear to $F1_2$ and $F1_1$ respectively. The corresponding constraint space comprises three constraints – $C2_1$, $C2_2$, and $C2_3$, which are not all coplanar but share the same intersection point.

A look at relationships between the freedoms of the two chains shows the intent behind the architecture of this mechanism. By connecting two chains that have collinear pitch and yaw freedoms, this mechanism serves as a parallel kinematic articulated wrist mechanism as reflected by the nominal constraint and freedom spaces shown in Fig. 8d. The mechanism's constraint space is the same as that of the first chain because all three of the second chain's constraints are redundant. Therefore, the mechanism's freedom space, in its nominal configuration, is therefore also identical to that of the first chain. However, some of the important geometric relationships that make this possible no longer hold in the displaced configuration.

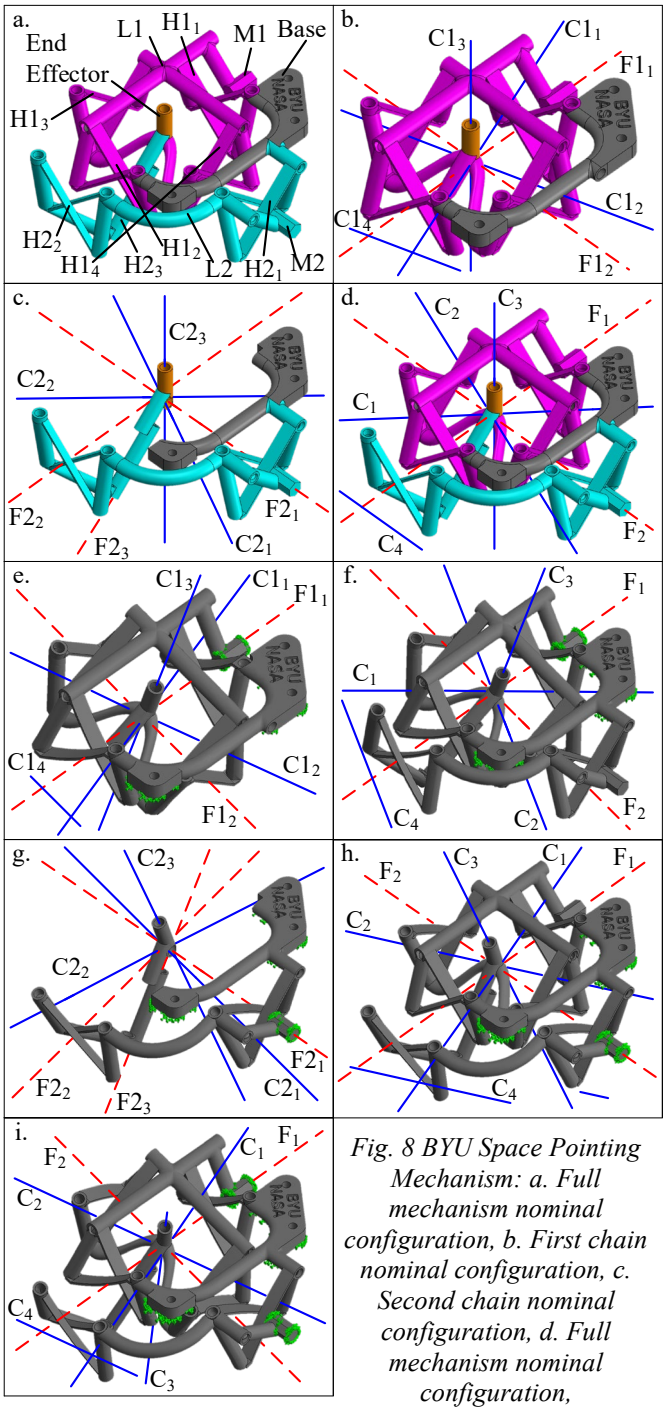

Fig. 8 BYU Space Pointing Mechanism: a. Full mechanism nominal configuration, b. First chain nominal configuration, c. Second chain nominal configuration, d. Full mechanism nominal configuration, e. First chain after rotation about $F1_1$, f. Full mechanism after single rotation about F_1, g. Second chain after rotation about $F2_1$, h. Full mechanism after single rotation about F_2, i. Full mechanism after both rotations

Copyright © 2020 ASME

The constraint and freedom spaces of the first chain after a single rotation about $F1_1$ are shown in Fig. 8e. Freedom $F1_2$ rotates along with the End Effector and the two freedoms maintain the same point of intersection as well as their orthogonal relationship. The plane composed of the two freedoms also remains orthogonal to the central axis of the End Effector. As expected, the constraint space of the chain also rotates about $F1_1$ but maintains all of the same relationships as in the nominal configuration.

The constraint and freedom spaces for the entire mechanism after a single rotation about F_1 are shown in Fig. 8f. While the second chain must also displace in order for this configuration to be possible, this displacement is almost entirely allowed by $H2_2$. This means that the freedom and constraint spaces of the second chain do not change significantly from the nominal configuration. As in the case of the nominal configuration, the mechanism's constraint and freedom spaces are dictated by the corresponding spaces of the first chain. Therefore, the mechanism appears to remain an articulated wrist mechanism. However, an important result of this rotation is that F_2 (dictated by $F1_2$) is no longer collinear to $F2_1$, which is still the axis of rotation of the actuator connected to the second chain. Given this, for the second rotation $F2_1$ to happen, the flexural pivots $H1_3$ and $H1_4$ would have to have finite compliance in their DoC. Analogously, flexural pivots $H2_2$ and $H2_3$ would also need to have finite compliance about their DoCs in order for a rotation about $F1_2$ to be possible.

A similar issue occurs when the second chain rotates about $F2_1$ first. The freedom and constraint spaces of the second chain after this rotation are shown in Fig. 8g. Both $F2_2$ and $F2_3$ have rotated about $F2_1$ but all three freedoms still intersect at the same point. As a result, both spaces do not change significantly from the nominal configuration. The constraint and freedom spaces for the entire mechanism after a single rotation about $F2_1$ are shown in Fig. 8h. The freedom and constraint spaces of the first chain will not change from the nominal configuration because the displacement in the chain is almost entirely provided by pivots $H1_3$ and $H1_4$. Since the constraint and freedom spaces for both chains are effectively identical to those in the nominal configuration, the mechanism constraint space for this displaced configuration is also effectively identical to that of the nominal configuration. From this displaced configuration ($F2_1$), if a next rotation about F_1 were to occur, then $F1_2$ would no longer be collinear to $F2_1$. This rotation about F_1 would not be possible unless the flexural pivots $H1_3$ and $H1_4$ have finite compliance in their DoCs.

This analysis shows that if this mechanism were to be composed entirely of joints that are ideal (i.e. completely rigid in their DoCs), it would only be able to rotate along one of the two rotational DoFs at a time. However, this mechanism behaves as an articulated wrist mechanism where both pitch and yaw can be simultaneously actuated if pivots $H1_3$, $H1_4$, $H2_2$, and $H2_3$ have finite compliance along certain DoCs. This shows how intentional use of compliance can enable functionality that would otherwise not be possible. One possible representation of the constraint and freedom spaces of this mechanism after rotations about $F1_1$ and $F2_1$ is shown in Fig. 8i.

In this mechanism, while the nature and location of the pitch and yaw freedom lines does not appear to change due to mechanism kinematics, these lines may still drift due to small but finite deformations along DoCs of some of the flexural pivots. This can lead to these freedom lines not intersecting as well. However, these deviations should be relatively small compared to the size of the mechanism. The range of motion of this mechanism is tied to the amount of finite compliance incorporated in certain DoCs of the flexural pivots. This compliance will also reduce load bearing and transmission capabilities because loading will cause increasing deformation of the flexural pivots in their DoCs. One instance of this mechanism [10], made monolithically out of titanium, provided a modest range of motion (~ 15° cone) with moderate to high stiffness expected in its DoCs. This was meant for a jet pointing application involving large loads but small ranges of motion.

3. CONCLUSION

The motion attributes of all six mechanisms are summarized in Table 1. Of these, the nature (i.e. purely rotational or screw) and location (static or drifting) of the two rotational DoFs in the nominal and displaced configurations are two key attributes that allow for a functional categorization of the mechanisms. Mechanisms that provide purely rotational pitch and yaw DoFs that do not translate over their workspace, such as the Dual Arch and Agile Eye mechanisms, can be used in a wide range of applications that require tracing a constant radius spherical section. It is difficult to find or design a parallel kinematic articulated wrist mechanism that is able to trace an entire hemisphere; mechanisms belonging to this category can typically achieve only a portion of a hemisphere limited by singularities and/or link collision. This is an important area of future investigation and innovation.

Mechanisms in which the nature of the pitch and yaw DoFs change such as the OmniWrist V and III are limited to use in applications that either do not require a workspace with constant radius or can compensate for this nonideal behavior. Mechanisms in which the locations of the pitch and yaw DoFs can drift such as the FlexDex and BYU Space Pointing mechanisms are also similarly limited in their applications.

The FlexDex and BYU Space Pointing mechanisms also stand apart for their intentional use of compliance, which enables functionality that may be difficult to achieve using ideal links and joints. However, this approach also leads to tradeoffs, including potential drifting of the location of their rotational DoFs, as noted above. Location of DoFs for such mechanisms can be both orientation-dependent and load-dependent because of their links and joints may deform under loading. Compliance also impacts the mechanism's range of motion and load bearing and transmission capabilities.

Another important design strategy utilized by many of the reported mechanisms is over-constraint, which can be used for several reasons. One reason is to provide the capability for ground-mounted actuation for each DoF, as is the case for the Agile Eye mechanism. Another reason is to increase the load

 Copyright © 2020 ASME

bearing capabilities as can be done for the OmniWrist V and III, in which additional serial chains can be added to improve stiffness. Load transmission capability can similarly be improved and can also provide the ability to over-actuate a DoF (e.g. providing independent actuators to all four of the OmniWrist III mechanism's serial chains). In each of these scenarios, over-constraint is only possible when the additional constraints are redundant throughout the mechanism's range of motion. Great care must be taken when utilizing overconstraint to ensure that this condition is met. This can be done by intentionally introducing small clearances into joints or by utilizing compliance. For example, compliance is introduced in the FlexDex mechanism to ensure that constraints remain redundant. Clearance in joints leads to lack of motion precision in the mechanism. These are typical tradeoffs when using over-constraint.

Finally, it is important to note the diversity in mechanisms that can produce the same mechanism freedom space. For example, both the Dual Arch and FlexDex mechanisms share similar freedom spaces when the FlexDex mechanism's compliant strips are assumed compliant in torsion. The OmniWrist III and V mechanisms also have similar freedom spaces because each of the OmniWrist III's serial chain provides a constraint space that is the same as the combined constraint space of the OmniWrist V's outer and central serial chains. Despite having similar freedom spaces, each mechanism provides a unique set of performance tradeoffs that makes it better suited for different applications. Thus, if a certain freedom space is desirable in mechanism synthesis, identifying multiple individual serial chains or combinations thereof that provide identical constraint spaces may lead to distinct mechanisms with different performance tradeoffs.

ACKNOWLEDGEMENT

Revanth Damerla was supported by a National Science Foundation Graduate Research Fellowship during this research.

Table 1 Motion Attributes of the Articulated Wrist Mechanisms
(N –Nominal Configuration, D –Displaced Configuration, R – with ideal links and joints, F – with some compliance)

Mechanism	Total Number of DoFs	Location of Pitch and Yaw DoFs	Nature of Pitch and Yaw DoFs	Load Bearing Capability	Load Transmission Capability
Dual Arch	4 (N, D)	On Central Axis (N, D)	Rotational (N, D)	High	High
Agile Eye	3 (N, D)	On Central Axis (N, D)	Rotational (N, D)	Moderate	Moderate
OmniWrist V	2 (N, D)	On Central Axis (N, D)	Rotational (N), Screw (D)	High	High
OmniWrist III	2 (N, D)	On Central Axis (N, D)	Rotational (N), Screw (D)	Moderate	Moderate
FlexDex	3 (N), 2 (DR), 4 (DF)	On Central Axis (N), Can Drift (DF)	Rotational (N, D)	Low	Low
BYU Space Pointing Mechanism	2 (N), 1 (DR), 2 (DF)	On Central Axis (N), Can Drift (DF)	Rotational (N, D)	Moderate	Moderate

Copyright © 2020 ASME

REFERENCES

[1] Awtar, S., Trutna, T. T., Nielsen, J. M., Abani, R., and Geiger, J., 2010, "FlexDex™: A Minimally Invasive Surgical Tool with Enhanced Dexterity and Intuitive Control," *ASME Journal of Medical Devices*, **4**(3), pp. 1–8.

[2] Awtar, S., and Nielsen, J., 2019, "Parallel Kinematic Mechanisms with Decoupled Rotational Motions", US 10,405,936 B2.

[3] Schoepp, H., 2013, "Axial Surgical Trajectory Guide," US 2013/0066334 A1.

[4] Vischer, P., and Clavel, R., 2000, "Argos: A Novel 3-DoF Parallel Wrist Mechanism," *International Journal of Robotics Reearch.*, **19**(1), pp. 5–11.

[5] Rosheim, M. E., 1989, *Robot Wrist Actuators*, Wiley, NY.

[6] Rosheim, M. E., 1994, *Robot Evolution: The Development of Anthrobotics*, Wiley, NY.

[7] Gosselin, C. M., and Hamel, J. F., 1994, "Agile Eye: A High-Performance Three-Degree-of-Freedom Camera-Orienting Device," *Proceedings of IEEE International Conference on Robotics and Automation*, pp. 781–786.

[8] Gosselin, C. M., St. Pierre, E., and Gagné, M., 1996, "On the Development of the Agile Eye," *IEEE Robotics & Automation Magazine*, **3**(4), pp. 29–37.

[9] Rosheim, M. E., and Sauter, G. F., 2002, "New High-Angulation Omni-Directional Sensor Mount," *Proceedings of SPIE, Free-Space Laser Communication and Laser Imaging II*, **4821**, pp. 163-174.

[10] Merriam, E. G., Jones, J. E., Magleby, S. P., and Howell, L. L., 2013, "Monolithic 2 DOF Fully Compliant Space Pointing Mechanism," *Mechanical Sciences.*, **4**(2), pp. 381–390.

[11] Hopkins, J. B., Panas, R. M., Song, Y., and White, C. D., 2017, "A High-Speed Large-Range Tip-Tilt-Piston Micromirror Array," *Journal of Microelectromechanical Systems*, **26**(1), pp. 196–205.

[12] McNamara, I. E., Toombs, N. J., Kim, J., Mcnamara, D. P., and Rapp, N. L., 2019, "Autonomous Fire Locating And Suppression Apparatus And Method", US 2019/0054333 A1.

[13] Blanding, D. L., 1999, *Exact Constraint: Machine Design Using Kinematic Principles*, ASME Press, NY.

[14] Hunt, K. H., 1979, *Kinematic Geometry of Mechanisms*, Oxford University Press, USA.

[15] Zhao, J., Feng, Z., Chu, F., and Ma, N., 2014, *Advanced Theory of Constraint and Motion Analysis for Robot Mechanisms*, Elsevier Inc.

[16] Hopkins, J. B., and Culpepper, M. L., 2010, "Synthesis of Multi-Degree of Freedom, Parallel Flexure System Concepts via Freedom and Constraint Topology (FACT) - Part I: Principles," *Precision Engineering*, **34**(2), pp. 259–270.

[17] Hopkins, J. B., and Culpepper, M. L., 2010, "Synthesis of Multi-Degree of Freedom, Parallel Flexure System Concepts via Freedom and Constraint Topology (FACT). Part II: Practice," *Precision Engineering*, **34**(2), pp. 271–278.

[18] Awtar, S., 1998, *Synthesis and Analysis of Parallel Kinematic XY Flexure Mechanisms*, Massachusetts Institute of Technology.

[19] Rosheim, M. E., 2017, "Robot Manipulator with Spherical Joints," US 9,630,326 B2.

[20] Rosheim, M. E., 2000, "Robotic Manipulator," US 6,105,455.

[21] Rosheim, M. E., 2003, "Robotic Manipulator," US 6,658,962 B1.

[22] Kong, X., and Gosselin, C. M., 2004, "Type Synthesis of 3-DOF Spherical Parallel Manipulators Based on Screw Theory," *ASME Journal of Mechanical Design*, **126**(1), pp. 101–108.

[23] Hess-Coelho, T. A., 2007, "A Redundant Parallel Spherical Mechanism for Robotic Wrist Applications," *ASME Journal of Mechanical Design*, **129**(8), pp. 891–895.

[24] Bonev, I. A., Chablat, D., and Wenger, P., 2006, "Working and Assembly Modes of the Agile Eye," *Proceedings - IEEE International Conference on Robotics and Automation*, pp. 2317–2322.

Copyright © 2020 ASME